Molecular Dynamics Study of the Structure and Thermophysical Properties of Model sI Clathrate Hydrates

A. A. Chialvo,*,†,‡ Mohammed Houssa,‡ and P. T. Cummings§,||

High-Temperature Aqueous Chemistry Group, Chemical and Analytical Sciences Division, and Chemical Technology Division, Oak Ridge National Laboratory, Oak Ridge, Tennessee 37831-6110, and Departments of Chemical Engineering, Chemistry, and Computer Science, University of Tennessee, Knoxville, Tennessee

Received: July 16, 2001; In Final Form: October 8, 2001

We performed isothermal−isobaric molecular dynamics simulations to study the effects of host−guest asymmetries on the thermophysical and structural properties of methane and carbon dioxide sI clathrate hydrates. In particular, we analyzed the effect of the strength of the host−guest interactions in realistic molecular descriptions of the host intermolecular potentials, the effect of the type of water intermolecular potential, and the degree of cage occupancy on the resulting properties of the hydrates. Finally, we used the simulation results to interpret the limitations and implications of the main assumptions behind the original vdWP theory of clathrates and its current modifications, which are used in the modeling of hydrate phase equilibria.

Introduction

Gas (clathrate) hydrates represent an intriguing class of nonstoichiometric inclusion compounds showing that, given the right conditions, water can form (solid) solutions with hydrophobic molecules. The resulting solid solutions (hydrates) consist of a crystalline host lattice (water solvent) that encloses the guest (usually a natural gas component). The gas hydrate structure differs from that of the corresponding ice and depends on the nature of the solute guest. The empty hydrate lattice, consisting of water alone, is thermodynamically unstable, i.e., it owes its existence to the hydrogen-bond stabilization resulting from the presence of the trapped solute under suitable state conditions.[1] In fact, the hydrophobic guest makes it possible for the water to be solid under conditions such that water would otherwise be a liquid.

The basic hydrogen-bonded water cavity is the pentagonal dodecahedron, i.e., a polyhedron with 12 pentagonal faces, which is able to accommodate just one guest solute. An arrangement of these polyhedra linked together by their vertices form the so-called structure I (sI). Because these dodecahedra cannot pack tightly, the unit cubic cell of sI is formed from two dodecahedra and six tetrakaidecahedra (a polyhedron with 12 pentagonal and two hexagonal faces). Thus, the cell contains 46 water molecules and can hold up to 8 small gas molecules (i.e., a maximum hydration number of 5.75 for solutes with an effective size smaller than 5.2 Å).

Gas hydrates occur naturally in sediments under pressure and temperature conditions of permafrost (polar) regions and in outer continental margins (deep ocean regions).[2] Even though other gases such as light hydrocarbons and carbon dioxide can form gas hydrates provided that the conditions are appropriate, methane hydrates are the most common naturally occurring type of clathrate. Methane is typically the main constituent of these hydrates, with a 10-fold higher energy density (STP volume of gas per volume of sediment/rock) than other nonconventional gas sources, such as coal beds, and a 2−5 times larger energy density than conventional natural gas.[2]

Two important factors make methane hydrates a potentially attractive clean energy resource, namely, the size of the methane fields in the form of hydrates in shallow seafloor sediments (within 1.5 miles of sea level) and the wide geographical distribution of the gas hydrates.[3] Conservative estimates indicate that the worldwide amount of methane hydrates is of the order of 10 Tton, i.e., about twice the carbon found in all fossil fuels on earth.[4] Moreover, the use of natural gas from hydrates as a source of energy, as opposed to coal or petroleum, can help mitigate greenhouse gas emissions, provided that the release of methane into the atmosphere is prevented. In fact, the stability of gas hydrates is strongly affected by changes in the pressure and/or temperature of the shallow seafloor where they form. Thus, any increase in temperature and/or decrease in pressure has the potential to destabilize the hydrates, resulting in decomposition and consequent release of methane into the atmosphere. Considering that methane exhibits a greenhouse effect approximately 20 times stronger than that of carbon dioxide,[5] any substantial additional methane release from the decomposition of hydrates will contribute positive feedback in the global warming cycle, which eventually could result in a so-called runaway greenhouse effect.[6] Therefore, although methane hydrates represent a significant untapped hydrocarbon source,[3] their physical chemistry under seafloor conditions is not yet well understood and becomes an important factor hindering large-scale exploitation of these potential energy sources as a result of environmental concerns.[7]

Broadly speaking, our current understanding of clathrate behavior hinges on the cell theory, proposed half a century ago

* To whom correspondence should be addressed (e-mail chialvoaa@ornl.gov, Fax 865-574-4961).

† Chemical and Analytical Sciences Division, Oak Ridge National Laboratory.

‡ Department of Chemical Engineering, University of Tennessee.

§ Departments of Chemical Engineering, Chemistry, and Computer Science, University of Tennessee.

|| Chemical Technology Division, Oak Ridge National Laboratory.

10.1021/jp012735b CCC: $22.00
Published on Web 12/11/2001

by van der Waals,[8,9] who assumed that the encaging of guest molecules in a metastable empty host structure (the so-called β-modification) leads subsequently to a stable configuration (the α-modification). This theory encompasses in principle three clear assumptions within the framework of classical statistical mechanics: (a) the host cavities exclude multiple guest occupancy, (b) the guest−guest interactions can be neglected, and (c) the guest molecules (host occupancy) do not affect the contribution of the β-structure to the hydrate partition function. On the basis of these assumptions, van der Waals[9] derived a simple expression for the hydrate Helmholtz free energy, written here explicitly for a single guest and a single cavity type, i.e.

$$A^{H}/kT = (A^{\beta}/kT)\exp\left\{-\left[\frac{N!}{(N\theta)![N(1-\theta)]!}\right]h_g(T)^{N\theta}\right\} \quad (1)$$

where β denotes the empty host, Nm is the number of host molecules forming N cavities, $\theta = N_g/N$ is the degree of occupancy of the cavity, and $h_g(T)$ is the partition function of an encaged guest molecule. (Note that, although we have used the original nomenclature of van der Waals,[9,10] an alternative notation is frequently used in which N is replaced by νN, where $m = \nu^{-1}$ is the number of solvent molecules forming the cavity.[1,11]) From eq 1, the corresponding species chemical potentials become

$$\mu_g^{H} = kT\ln[\theta/(1-\theta)] - kT\ln h_g(T) \quad (2)$$

$$\mu_w^{\alpha} = \mu_w^{H} = \mu_w^{\beta} + (kT/m)\ln(1-\theta) \quad (3)$$

To make practical use of eq 1, van der Waals estimated $h_g(T)$ by introducing two additional assumptions: (d) the guest molecules behave as ideal-gas free rotors, and (e) the potential energy of the guest molecule is represented by a spherically symmetric cavity potential $\varphi(r)$ centered at the center of the host cage.[12] Consequently, $h_g(T) = kT\Phi(T)\,C(T)$, where $\Phi(T)$ is the ideal-gas contribution to the guest partition function and $C(T)$ is the so-called Langmuir constant

$$C(T) \equiv (4\pi/kT)\int_0^{\mathscr{R}} \exp[-\varphi(r)/kT]r^2\,dr \quad (4)$$

so that the fractional occupancy becomes

$$\theta = C(T)f/[1 + C(T)f] \quad (5)$$

where f is the fugacity of the guest in the hydrate.

Most published molecular-based work on hydrates has been directed toward testing the validity of the hypotheses behind the vdWP model. These simulations have typically involved simple, nonpolarizable water intermolecular potential models with rigid geometries such as the SPC model[13] and the TIP4P model[14] or flexible geometries such as the SPC−F model,[15] as well as one-site spherically symmetric solutes typically described as Lennard-Jones atoms. The main thrust behind these simulations has been the explicit description of the three water sites (the oxygen and two hydrogen sites), with little emphasis being placed on the actual solute geometry and the corresponding molecular asymmetry of the resulting intermolecular potential. Even though most simulation studies of hydrates have been based on rather simple host−guest models and small samples,[16−18] they have demonstrated the ability of these molecular tools to offer microscopic insights into the clathrate phenomena.

TABLE 1: Intermolecular Potential Parameters for the Water Models Used in This Study

model	ϵ_{OO}/k (K)	σ_{OO} (Å)	q_O (e)	l_{OH} (Å)	∠HOH (°)	μ(D)
SPC	78.23	3.166	−0.410	1.0	109.5	2.27
SPC/E	78.23	3.166	−0.4238	1.0	109.5	2.35
TIP5P[a]	80.75	3.120	−0.2410	0.9572	104.5	2.29

[a] Two additional positive charges are located in a perpendicular plane to the HOH plane, forming an angle of $\angle qOq = 109.5°$ with an O−q distance of $l_{Oq} = 0.7$ Å.[20]

TABLE 2: Intermolecular Potential Parameters for the Lennard-Jones Solute Models

model	ϵ_{OO}/k (K)	σ_{OO} (Å)
CO_2	232.0	3.643
CH_4	148.0	3.730

A more realistic representation of host−guest interactions is a crucial factor for the successful molecular-based description of condensed fluids, as the molecular asymmetry (difference between solute−solvent and solvent−solvent intermolecular forces) between species in solution ultimately dictates the phase equilibria of the system. In addition, a stringent test of the hypothesis behind the vdWP hydrate theory is only possible if we are able to realistically describe not only the host−host but also the host−guest and the guest−guest interactions.

In this investigation, we analyze, by molecular dynamics simulation under isobaric−isothermal conditions, the thermophysical and structural properties of methane and carbon dioxide clathrate hydrates, as described by accurate and realistic multisite intermolecular potential models. We compare these results with those corresponding to the solutes described by spherically symmetric Lennard-Jones potentials to test underlying hypotheses behind hydrate modeling. In particular, we analyze the effects of the strength of the host−guest interactions, the type of water potential, and the degree of cage occupancy on the resulting properties of the hydrate. Finally, we use the simulation results to interpret the main assumptions behind the original vdWP theory of clathrates, as well as the numerous modifications currently in use for the modeling of hydrate phase equilibria.

Intermolecular Potential Models

This study involves three water models, the SPC,[13] the SPC/E,[19] and the TIP5P[20] models. The three models incorporate a Lennard-Jones potential for the oxygen−oxygen interactions and a Coulomb model for the electrostatic interactions between all charged sites. On one hand, for the two variations of the simple point-charge model (SPC and SPC/E) we know the vapor−liquid phase envelope and the corresponding critical conditions.[21,22] On the other hand, in contrast to the planar SPC's geometry, the TIP5P model involves a nonplanar geometry and gives the best representation yet (for a nonpolarizable model) of the isobaric density profile at low temperature, in particular, the description of the density maximum at the correct temperature. In Table 1, we display the potential parameters for these three water models.

For the CH_4 species, we have chosen both the simplest Lennard-Jones representation according to the OPLS parametrization[23] and the five-site (rigid geometry) model given by set VII of Williams' parametrization.[24] The latter provides the most accurate representation of the structure and thermophysical properties,[25,26] as well as the vapor−liquid equilibrium.[27] In Table 2, we display the Lennard-Jones parameters for the OPLS methane model.

TABLE 3: Intermolecular Potential Parameters for Methane According to Set VII of Williams' Model

interaction	$A_{\alpha\beta}/k$ (K Å^6)	$B_{\alpha\beta}/k$ (K)	$C_{\alpha\beta}$ (Å^{-1})
CC	-2.541×10^5	3.115×10^7	3.60
CH	-6.441×10^4	5.536×10^6	3.67
HH	-1.625×10^5	1.32×10^6	3.74

TABLE 4: Intermolecular Potential Parameters for Williams' Methane as Translated to the Lennard-Jones Counterpart

interaction	$\epsilon_{\alpha\beta}/k$ (K)	$r_m^{\alpha\beta}$ (Å)	$\sigma_{\alpha\beta}$ (Å)
CC	48.72	3.779	3.351
CH	20.55	3.435	3.024
HH	6.79	3.268	2.868

TABLE 5: Intermolecular Potential Parameters for Carbon Dioxide According to Harris−Yung's EPM2 Rigid Model

interaction	$\epsilon_{\alpha\beta}/k$ (K)	$\sigma_{\alpha\beta}$ (Å)
CC	28.129	2.757
CO	47.588	2.892
OO	80.507	3.033

The Williams model for methane is based on a rigid geometry, with a bond length $l_{CH} = 1.04$ Å (although Murad et al.[25] and Habenschuss et al.[26] have used 1.026 Å instead) and a bond angle $\vartheta_{H-C-H} = 109.5$, and exponetial-6-type potentials for the site−site CC, CH, and HH interactions, i.e.

$$\phi_{ij}(r_{ij}) = \sum_{\alpha,\beta}^{5} \phi_{\alpha\beta}(r_{ij}^{\alpha\beta}) = \sum_{\alpha,\beta}^{5} B_{\alpha\beta} \exp(-C_{\alpha\beta} r_{ij}^{\alpha\beta}) + A_{\alpha\beta}/(r_{ij}^{\alpha\beta})^6 \quad (6)$$

where the coefficients of this expression are given in Table 3.

For the methane−water nonelectrostatic potential interactions, we adopted the standard Lorentz−Berthelot combining rules. For that purpose, we translated the exp-6 potential form into a Lennard-Jones-type potential by determining first the distances $\sigma_{\alpha\alpha}$ at which $\phi_{\alpha\alpha}(r=\sigma_{\alpha\alpha}) = 0$ and then the minimum value $\phi_{\alpha\alpha}(r=r_m) = -\epsilon_{\alpha\alpha}$. These parameters are straightforwardly obtained by an iteration procedure as indicated in the Appendix and displayed in Table 4.

For the CO_2 species, we also analyzed its simplest Lennard-Jones description whose parameters were derived from the critical conditions of the model[28] and real fluid[29] and the three-site linear (rigid) geometry developed by Harris and Yung.[30] The latter, the rigid version of the EPM2 model (Table 5) with a bond length $l_{CO} = 1.149$ Å and a point charge $q_C = 0.6512e$, provides a remarkably accurate description of the vapor−liquid phase envelope and corresponding thermodynamic properties.

Simulation Methodology

All simulations were performed with a total of 432 (416, 400, 384, or 376) particles, including 64 (48, 32, 16, or 8) guests and 368 water (host) molecules, at $P = 5$ MPa and $T = 270$ K using a Nosé[31]−Andersen[32] approach. Thus, each system represents a total of eight sI hydrate unit cells, with either full host (64 guest molecules), three-quarter (48 guest molecules), one-half (32 guest molecules), one-quarter (16 guest molecules), or single occupancy (8 guest molecules). An additional simulation with only 4 guest molecules was performed just for comparison purposes to highlight the differences between the structure of a gas hydrate and its aqueous-gas solution counterpart.

The Newton−Euler equations of motion were integrated using 5th-order and 4th-order Gears' predictor−correctors[33] for the translational and rotational degrees of freedom, respectively, with a time step of 1.0 fs. All simulations were run for 800 ps, after an equilibration period of 200 ps, divided into blocks of 20 ps to assess the uncertainties of the calculated time averages according to the standard approach.[34]

The rigid-body orientations were described by the Evans−Murad quaternion formalism.[35] Long-ranged electrostatic interactions were handled by the molecular reaction field approach,[36] and nonelectrostatic interactions were truncated at a distance $r_c = 3.0\sigma_{OO}$ using the standard long-range pressure and configurational internal energy corrections.

The starting configurations for all simulations were based on the sI structural information from X-ray analysis of ethylene oxide hydrate by McMullan and Jeffrey,[37] i.e., for the location of the water oxygens and the center of mass of the guest molecules. The initial orientations for the water molecules were assigned at random, and subsequently, a short dynamics simulation let the water hydrogen atoms settle into the correct orientations consistent with the Bernal−Fowler rule[38] and zero dipole moment. This condition was achieved by allowing the water molecules to rotate about the oxygen atomss to minimize their configurational energy while freezing their translational degrees of freedom.

Simulation Results and Discussion

In Tables 6−9, we display and compare the thermodynamic properties of the hydrates as predicted by simulation. In each table, we compare the hydrates resulting from a microscopic description of the solute (guest) in three different water (host) models. The microstructure of the hydrate is described by the host's site−site radial distribution functions $g_{OO}(r)$, $g_{OH}(r)$, and

TABLE 6: Simulation Results for (Lennard-Jones) Carbon Dioxide Hydrates with $\theta = 1.0$ at $T = 270$ K and $P = 5$ MPa[a]

water	U_c (kJ/mol)[b]	U_{ww} (kJ/mol)[c]	U_{uu} (kJ/mol)[c]	U_{wu} (kJ/mol)[c]	ρ (g/cm^3)
SPC	-44.95 ± 0.02	-48.9 ± 0.06	-0.25 ± 0.01	-3.66 ± 0.01	1.153 ± 0.001
SPC/E	-44.80 ± 0.02	-48.7 ± 0.06	-0.26 ± 0.01	-3.75 ± 0.01	1.181 ± 0.001
TIP5P	-46.69 ± 0.02	-50.6 ± 0.06	-0.28 ± 0.01	-3.90 ± 0.01	1.225 ± 0.001

[a] The errors in U_c are smaller than those in U_{ww} because the number of interactions contributing to the first average is larger [$\sim(N_{water} + N_{gas})^2$] than the number contributing to the second average ($\sim N_{gas}^2$). [b] Per mole of mixture. [c] Per mole of water.

TABLE 7: Simulation Results for (Lennard-Jones) Methane Hydrates with $\theta = 1.0$ at $T = 270$ K and $P = 5$ MPa

water	U_c (kJ/mol)[a]	U_{ww} (kJ/mol)[b]	U_{uu} (kJ/mol)[b]	U_{wu} (kJ/mol)[b]	ρ (g/cm^3)
SPC	-43.23 ± 0.02	-47.7 ± 0.06	-0.18 ± 0.01	-2.85 ± 0.01	0.920 ± 0.001
SPC/E	-44.06 ± 0.01	-48.6 ± 0.06	-0.20 ± 0.01	-2.99 ± 0.01	0.951 ± 0.001
TIP5P	-45.89 ± 0.02	-50.6 ± 0.06	-0.20 ± 0.01	-3.13 ± 0.01	0.987 ± 0.001

[a] Per mole of mixture. [b] Per mole of water.

TABLE 8: Simulation Results for (Harris−Yung) Carbon Dioxide Hydrates With $\theta = 1.0$ at $T = 270$ K and $P = 5$ MPa

water	U_c (kJ/mol)[a]	U_{ww} (kJ/mol)[b]	U_{uu} (kJ/mol)[b]	U_{wu} (kJ/mol)[b]	ρ (g/cm^3)
SPC	-43.88 ± 0.06	-47.5 ± 0.06	-0.20 ± 0.01	-3.67 ± 0.01	1.139 ± 0.001
SPC/E	-44.26 ± 0.02	-47.4 ± 0.06	-0.21 ± 0.01	-3.68 ± 0.01	1.165 ± 0.001
TIP5P	-44.75 ± 0.07	-49.6 ± 0.06	-0.22 ± 0.01	-2.66 ± 0.01	1.146 ± 0.001

[a] Per mole of mixture. *b*Per mole of water.

TABLE 9: Simulation Results for (Williams) Methane Hydrates with $\theta = 1.0$ at $T = 270$ K and $P = 5$ MPa

water	U_c (kJ/mol)[a]	U_{ww} (kJ/mol)[b]	U_{uu} (kJ/mol)[b]	U_{wu} (kJ/mol)[b]	ρ (g/cm^3)
SPC	-43.19 ± 0.02	-46.39 ± 0.01	-0.130 ± 0.001	-3.00 ± 0.01	0.934 ± 0.001
SPC/E	-42.44 ± 0.02	-46.68 ± 0.01	-0.135 ± 0.001	-3.11 ± 0.01	0.955 ± 0.001
TIP5P	-44.48 ± 0.02	-48.80 ± 0.03	-0.143 ± 0.001	-3.23 ± 0.01	0.981 ± 0.001

[a] Per mole of mixture. [b] Per mole of water.

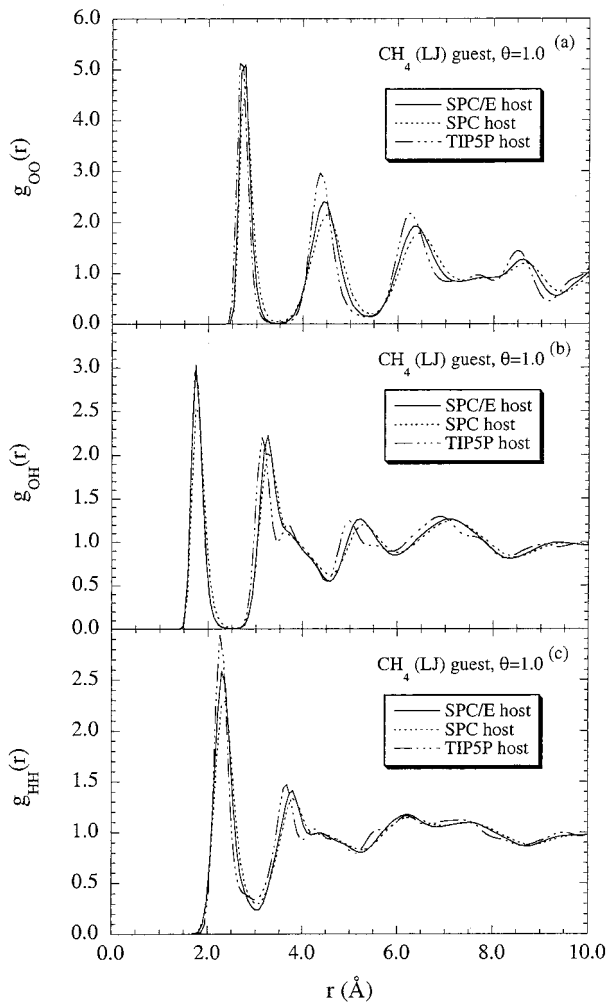

Figure 1. Comparison of the host (water) radial distribution functions for a methane hydrate at $T = 270$ K and $P = 5$ MPa where the guest is described by a simple atomic Lennard-Jones potential.

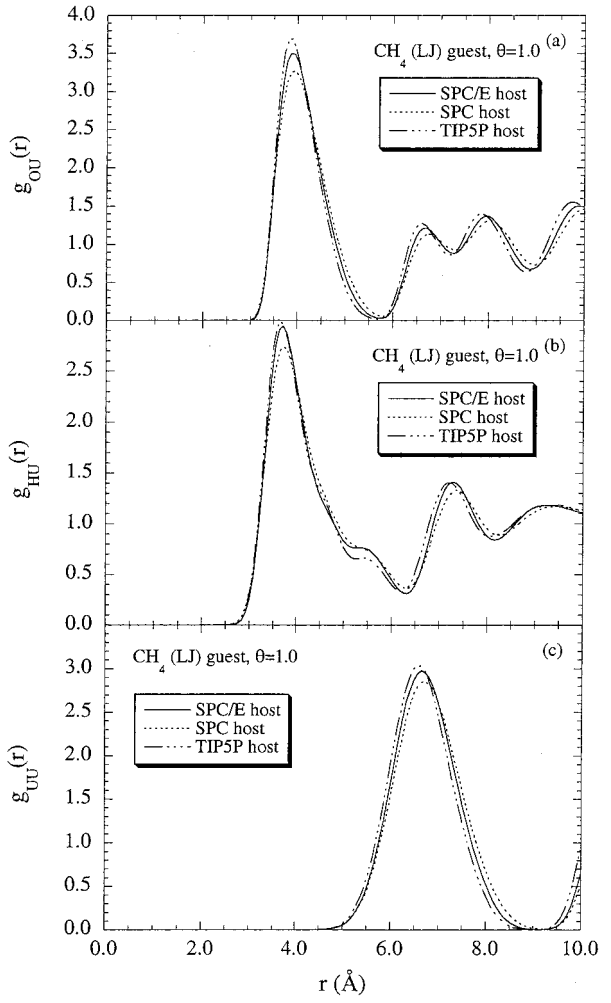

Figure 2. Comparison of the guest radial distribution functions for a methane hydrate at $T = 270$ K and $P = 5$ MPa where the guest is described by a simple atomic Lennard-Jones potential.

$g_{HH}(r)$ (Figures 1, 3, 5 and 7) and the guest's radial distribution functions $g_{OU}(r)$, $g_{HU}(r)$, and $g_{UU}(r)$ (Figures 2, 4, 6, and 8), where O and H are the corresponding host sites and U denotes the guest's center of mass, i.e., the carbon site in either guest species. The host structure exhibits the same features as ambient water,[39,40] such as the locations of the first two peaks of $g_{OO}(r)$ at about 2.78 and 4.5 Å, of the first two peaks of $g_{OH}(r)$ at 1.82 and 3.2 Å, and of the first two peaks of $g_{HH}(r)$ at 2.3 and 3.8 Å. Thus, these functions indicate the formation of tetrahedral structures, although much stronger than those observed in ambient water, as clearly shown by the higher and narrower correlation peaks (see Figure 10, where $\theta = 0.0625$ corresponds to a liquidlike rather than a hydrate structure).

On one hand, it becomes immediately obvious that, regardless of the type of guest molecule, the properties of the SPC and SPC/E hydrates are essentially the same (see also Figures 1−8 for the associated structural features). Note, however, that there is a clear isothermal−isobaric increase of the system density as we substitute the SPC by the SPC/E water as the hydrate's host, i.e., a manifestation of the larger SPC/E dipole moment (see the last column of Table 1). This density increase also translates into slightly stronger peaks in the corresponding host radial pair correlation functions (see Figures 1, 3, 5, and 7). On

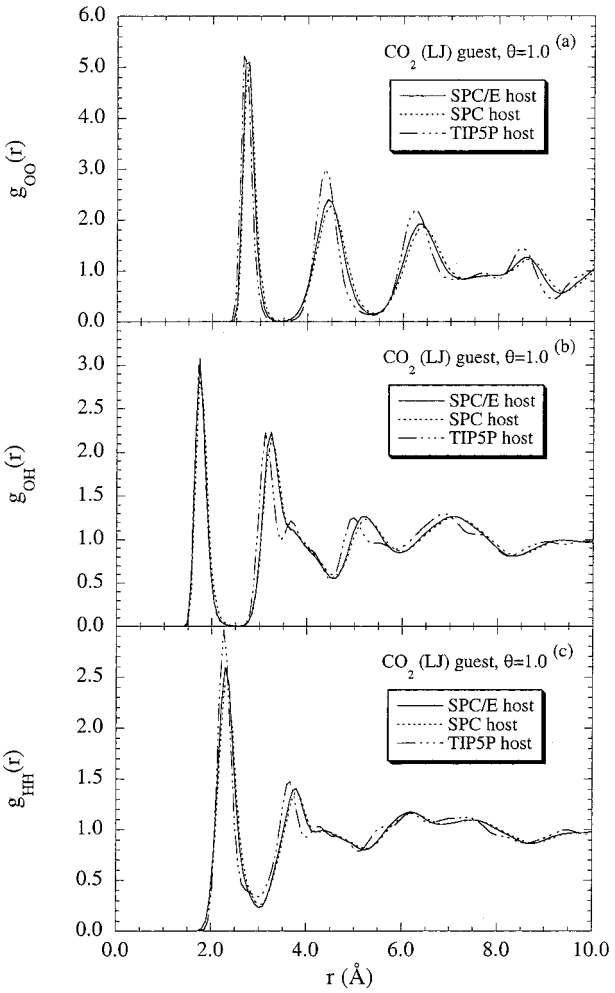

Figure 3. Comparison of the host (water) radial distribution functions for a carbon dioxide hydrate at $T = 270$ K and $P = 5$ MPa where the guest is described by a simple atomic Lennard-Jones potential.

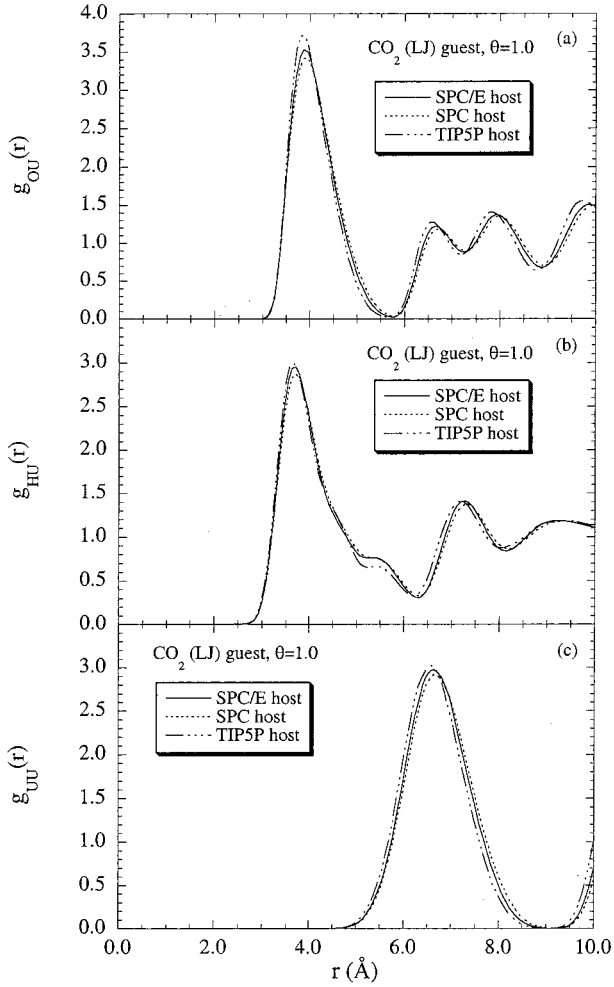

Figure 4. Comparison of the guest radial distribution functions for a carbon dioxide hydrate at $T = 270$ K and $P = 5$ MPa where the guest is described by a simple atomic Lennard-Jones potential.

the other hand, the substitution of the planar SPC water host by the nonplaner TIP5P water host induces larger isothermal−isobaric changes in the configurational energy, specifically from the host−host and host−guest interactions, and in the system's density. These changes cannot be ascribed solely to the differences in the dipole moment of the water models, $\mu_{SPC} < \mu_{TIP5P} < \mu_{SPC/E}$, but rather to the more favorable geometry of the TIP5P model to the formation of hydrogen bonds, which results in a more stable guest encapsulation. This is clearly manifested in the corresponding radial distribution functions (see Figures 1, 3, 5, and 7) and quantified in the more negative host−host configurational internal energy U_{ww}.

The effect of the nature/type/asymmetry of the enchathrated guest on the hydrate properties can be clearly analyzed by comparing results for the molecular and atomic descriptions of the guests. Whereas the Lennard-Jones size parameters for methane and carbon dioxide differ by 2%, the energy parameter for carbon dioxide is about 36% larger than that for methane. The latter difference clearly translates into stronger host−guest and guest−guest interactions than those for the methane counterpart (see Tables 6 and 7). Note also that, because of the single occupancy of the hydrate's cavity, "molecular" size does not have a strong effect on the properties.

Now, if we switch from the spherically symmetric (Lennard-Jones) guest to the more realistic molecular counterparts, we can analyze the effect of molecular asymmetry (shape, size, and range) on the properties of the resulting hydrates. Note that, even though methane is molecularly described by a five-site model (see Tables 3 and 4), it can be considered as a "globular" spherically symmetric molecule. In contrast, the three-site molecular description of carbon dioxide is definitely an elongated (linear) molecule, and therefore, these two guest molecules will interact rather differently with the host cavities and with one another (guest−guest interactions).

In terms of structure, both spherically symmetric (atomic) guest descriptions produce slightly stronger peaks for $g_{OU}(r)$ than do those from the molecular guest counterparts (compare Figures 2a and 6a and Figures 4a and 8a). More importantly, $g_{OU}(r)$ for the atomic guests exhibits a deeper first valley, $g_{OU}(r \approx 5.7-5.8\ \text{Å}) \approx 0$ and a stronger second peak, in drastic contrast with the molecular guests, i.e., $g_{OU}(r \approx 5.7-5.8\ \text{Å}) \approx 0.3-0.6$. In addition, $g_{HU}(r)$ for the "atomic" methane displays a more pronounced shoulder at the base of the first peak than does its molecular counterpart.

Perhaps more importantly, the results in Tables 6 and 8 indicate that the guest asymmetry (i.e., linear molecule versus sphere) affects the host configuration (compare the third columns of the above tables). In addition, the weaker nonspherically symmetric host−guest interactions of the three-site carbon dioxide (compare the fourth columns of the tables) translates into less dense hydrates (compare the last columns of the tables). Note, however, that these effects become milder when we

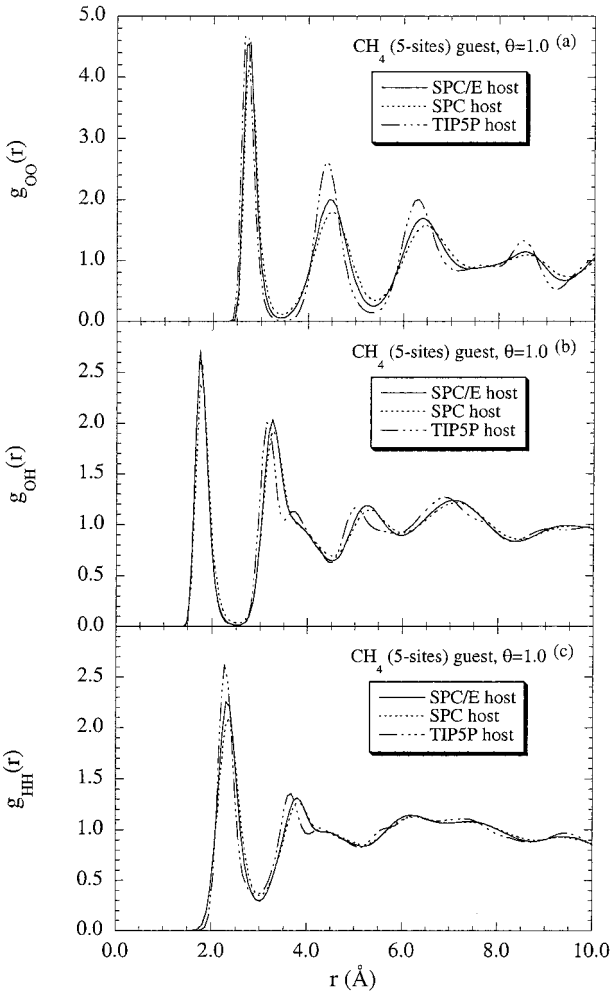

Figure 5. Comparison of the host (water) radial distribution functions for a methane hydrate at $T = 270$ K and $P = 5$ MPa where the guest is described by the five-site Williams potential.

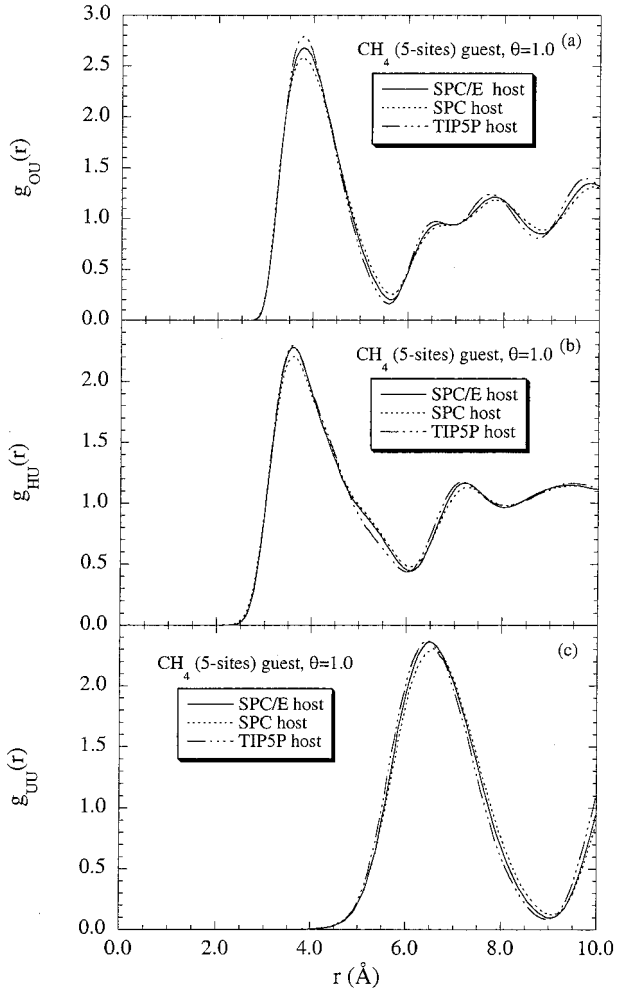

Figure 6. Comparison of the guest radial distribution functions for a methane hydrate at $T = 270$ K and $P = 5$ MPa where the guest is described by the five-site Williams potential.

consider the molecular asymmetry of methane, i.e., when the Lennard-Jones methane is compared with the five-site molecular methane.

The isobaric−isothermal contribution of host−host (water−water) interactions to the total configurational energy for various degrees of host occupancy indicates that $U_{ww}(T,P,\theta)$ is a monotonic function of the cell occupancy θ (Figure 9a). In fact, it exhibits a clear stabilization represented by a decrease of about 0.4 kJ/mol of water in $U_{ww}(T,P,\theta)$ when going from $N_g = 8$ ($\theta = 0.125$) to $N_g = 64$ ($\theta = 1.0$). From a microstructural viewpoint, this stabilization is clearly seen in the small but noticeable strengthening of the second peak of $g_{OO}(r)$ with increasing occupancy (Figure 10a), i.e., the peak that characterizes the tetrahedral nature of the hydrogen bonding.[41] That is a rather substantial energetic change that eventually invalidates the vdWP hypothesis regarding the independence of the host lattice free energy from the nature of the guest and degree of cell occupancy.[1] For comparison purposes, we should note that the difference of water chemical potential between the actual hydrate and the empty one, either $\mu_w^H - \mu_w^{MT} = -\Delta\mu'_w$ in Sloan's notation[11] or $\mu_w^\alpha - \mu_w^\beta$ in the original vdWP notation, is of the order of −1.0 kJ/mol of water under normal conditions.[42]

Moreover, the host−guest contribution to the total configurational energy exhibits a monotonic increase with the degree of host occupancy, so that $U_{wu}(T,P,\theta=1.0) \approx -3.67$ kJ/mol of water (Figure 9b). Once again, this behavior is manifested as stronger first peaks of the host−guest radial distribution functions (Figure 11a,b). Most importantly, the guest−guest interaction is not negligible as assumed in the vdWP theory; rather, it exhibits a clear quadratic dependence with the host occupancy (Figure 9c). For the maximum occupancy, the guest−guest contribution to the configurational energy in the carbon dioxide model hydrate is −0.2 kJ/mol of water, i.e., about one-fifth of the change of chemical potential ($\mu_w^\alpha - \mu_w^\beta$). Note that the guest−guest contribution is essentially the same for methane and carbon dioxide, i.e., it is not sensitive to the description of the intermolecular potential. However, there is a dramatic change in the strength of the first peak of $g_{UU}(r)$ with occupancy for the linear molecular description of carbon dioxide. That is, whereas there is no visible change for $1.0 \leq \theta \leq 0.5$, the strength of the first peak of $g_{UU}(r)$ increases from ~3 to ~8 for $0.5 \leq \theta \leq 0.125$ and then develops the expected behavior found in a dilute aqueous solution.

Final Remarks

If we compare the simulation results, in terms of the fundamental hypotheses of the vdWP theory (see the Introduction), with the apparently successful application of the vdWP theory (and its numerous modifications) to descriptions of the phase equilibria of gas clathrates, we find that these two items are at odds. On one hand, our results (and others from the available literature[16,17,43,44]) suggest that two of the main hypotheses of the vdWP theory are far from being appropriate

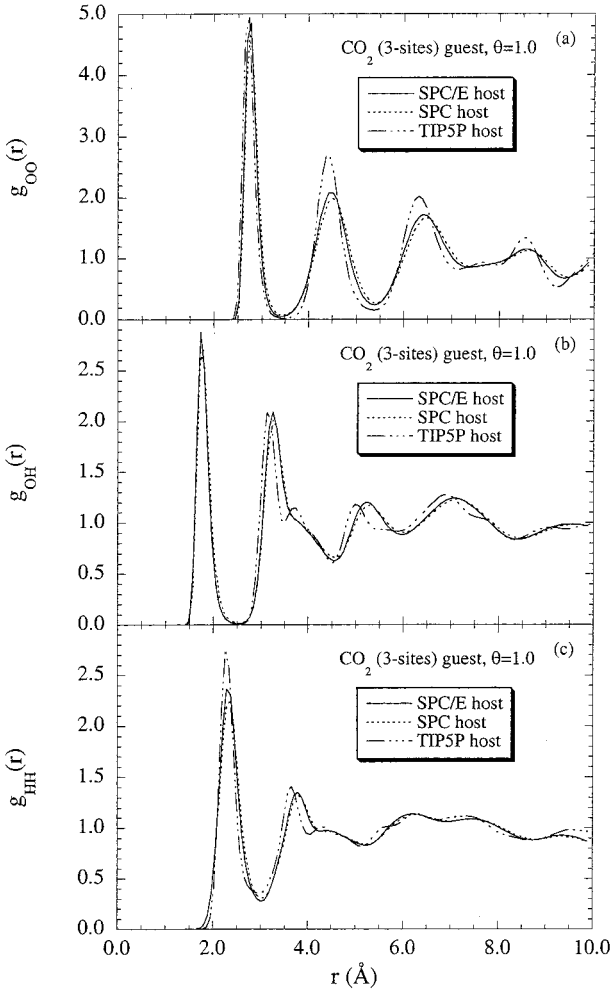

Figure 7. Comparison of the host (water) radial distribution functions for a carbon dioxide hydrate at $T = 270$ K and $P = 5$ MPa where the guest is described by the three-site Harris−Yung potential.

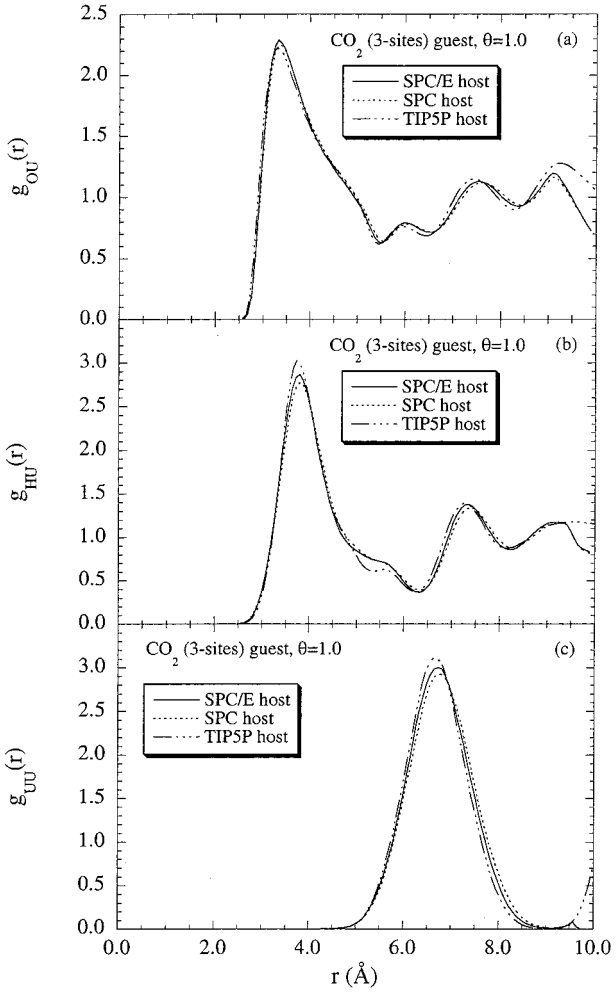

Figure 8. Comparison of the guest radial distribution functions for a carbon dioxide hydrate at $T = 270$ K and $P = 5$ MPa where the guest is described by the three-site Harris−Yung potential.

approximations, i.e., assumptions b and c in the Introduction are usually violated. Yet, this theory and its current modifications have become versatile tools for the regression of experimental data.[11,45]

In trying to solve the above dilemma, we must address a few issues associated with the validity of the assumptions embedded in the theory in light of the molecular dynamics results. A great deal of emphasis has been placed on determining the adequacy of the spherical cell approximation invoked in the calculation of the so-called cavity potential $\varphi(r)$ and the resulting Langmuir constant $C(T)$ (see eq 4). After the pioneering work of Tester[46] on accurate computation of the Langmuir constants, aimed at improving their estimations over those based on the Lennard-Jones Devonshire smooth cell approximation invoked in the vdWP theory, Holder and colleagues[47−50] suggested alternative modifications to the original vdWP theory to soften the inadequacies of the spherical approximation for $\varphi(r)$ and account for any possible lattice distortion. Even though these modifications might have improved the regression capability at the expense of introducing yet more adjustable parameters (the cell radius $\mathscr{R}$ and the aspherical correction coefficient Q^*), the resulting models and corresponding adjustable parameters tend to lose the original and clear physical picture of the clathrate solution. The success of the vdWP theory should not be a surprise if we consider that it involves a rather large number of adjustable parameters used in the regression of the equilibrium data, namely, four thermodynamic properties (the differences of properties between the empty lattice and pure water at the reference state $\Delta\mu_w^o$, Δh_w^o, Δv_w^o, and ΔC_{pw}^o), two parameters per cavity type (the cavity radius $\mathscr{R}$ and the number of water molecules m forming the cavity), and two to three force-field parameters per guest type (ϵ, σ, and a for a Kihara potential). (Note that, in principle and consistent with the vdWP theory, $\Delta\mu_w^o$, Δh_w^o, Δv_w^o, and ΔC_{pw}^o should be properties uniquely defined by the state conditions of the host, i.e., independent of the guest involved in the hydrate formation.) Thus, the 10 or so adjustable parameters defining the cavity potential and the host's reference-state properties are invariably determined ad hoc by regression of phase equilibrium data, and consequently, they are not uniquely defined (see, for example, Table 1 of Rodger[16] and Table 5.5 of Sloan[11]).

More recently, Sparks[51−53] revisited Tester's original work to analyze the inadequacy of the nearest-neighbor approximation used in the determination of the host−guest partition function and corresponding Langmuir constant for specific cavity types within the vdWP theory of hydrates. Although they explored several computational methods to evaluate accurately and efficiently the host−guest partition function, placing emphasis on the contributions farther away from the first host cell, they also, somewhat surprisingly, included the guest−guest interactions in their calculations. The latter is inconsistent with the definition of the Langmuir constant, i.e., the host−guest partition

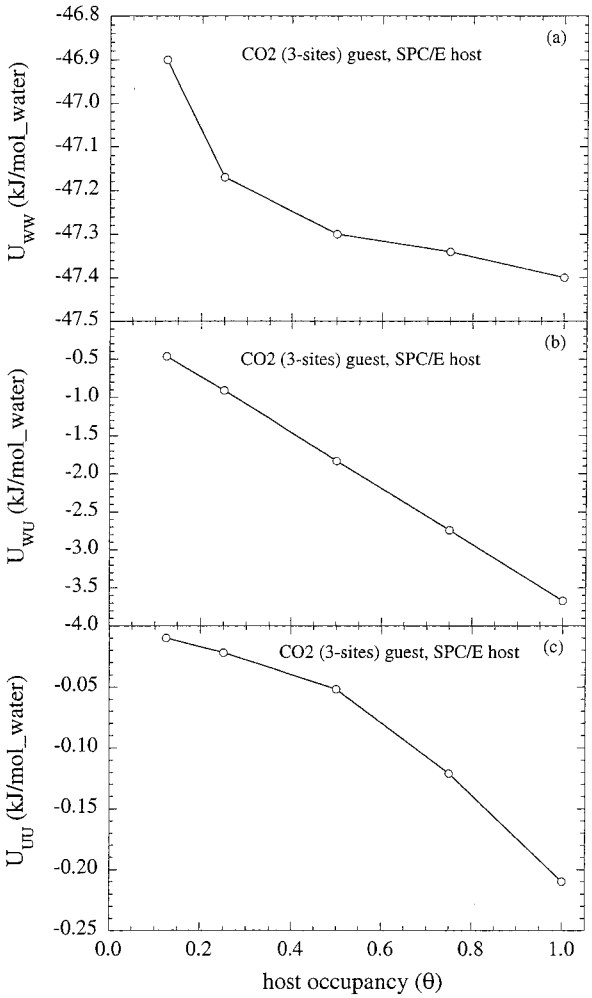

Figure 9. Isobaric−isothermal effect of host occupancy on the configurational internal energy of the carbon dioxide hydrate described by the Harris−Yung potential for the guest and the SPC/E model for the host.

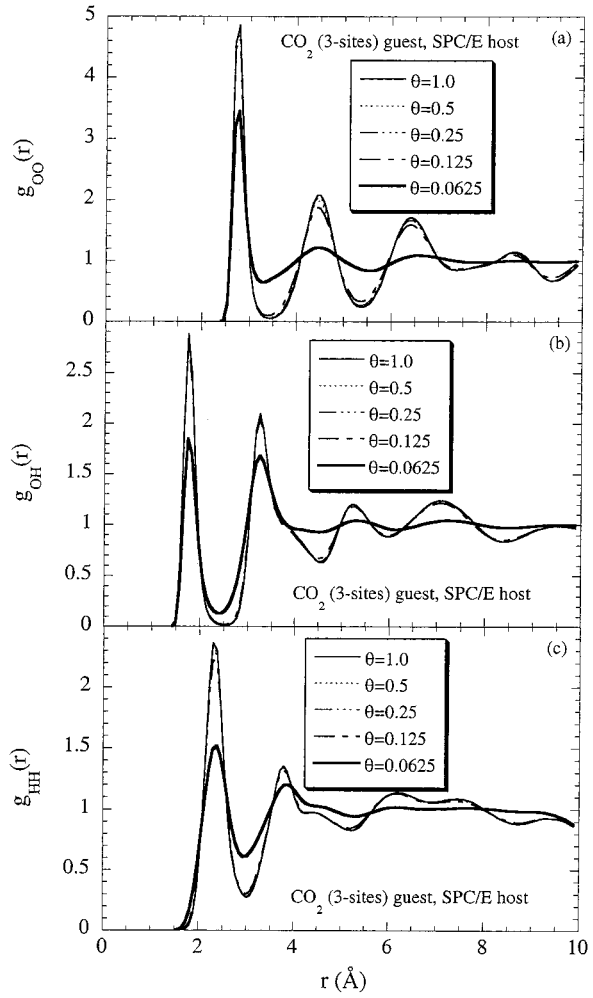

Figure 10. Isobaric−isothermal effect of host occupancy on the host microstructure for the carbon dioxide hydrate described by the Harris−Yung potential for the guest and the SPC/E model for the host.

function in the vdWP theory was not formulated to include the guest−guest interactions (assumption b in the Introduction).

Our molecular dynamics results (Tables 6−9 and Figures 1−12) suggest that many of the efforts spent in modifications of the original vdWP theory of hydrates have been misdirected in that they have wrongly targeted a more "accurate" or "realistic" calculation of the cavity potential (and, consequently, of the Langmuir constant). However, the fact of the matter is that the most obvious and frequent cause of failure of the vdWP theory (and its modifications) is the neglect of the small but significant guest−guest interactions. This simplifying assumption makes it possible to derive a flexible and simple theory for "ideal" gas clathrates that takes the simple form of Langmuir adsorption isotherms. In that sense, the vdWP theory can be considered the zeroth-order approximation (ideal lattice model) of a more general formalism. The general theory should explicitly include the guest−guest interactions (nonideal lattice model) in the same spirit as the Henry's Law lies in the development a fundamentally based theory of gas solubility.[54]

Unfortunately, most hydrates of industrial interest do involve nonnegligible guest−guest interactions, and consequently, their behavior cannot be analyzed within the framework of the vdWP theory. The fundamental reason is that the clathrate partition function in the vdWP theory does not involve guest−guest interactions. Explicit inclusion of the guest−guest partition function obviously alters the mathematical expression of the clathrate's Helmholtz free energy (see, for example, the derivations by Sitarski,[55] Belosludov and colleagues,[42] and Istomin[56]). In turn, this changes the functional relationships between the species fugacities, the state conditions, the host occupancy, and the host−guest and guest−guest interactions and, consequently, the resulting expressions for phase equilibrium calculations. These expressions cannot be obtained from or simply mapped to reparametrized ("more accurate" or "reinterpreted") Langmuir constants as is frequently done in engineering calculations.

In summary, most modifications to the vdWP theory designed to deal with real systems are fundamentally flawed. They can be regarded as data correlators that have been made more flexible at the expense of losing all molecular-based foundation, i.e., their adjustable parameters carry little physical meaning. It is also rather surprising that little attention has been paid to developments that explicitly invoke the guest−guest interactions,[55,42,56] which can be treated as natural extensions of the vdWP theory, i.e., $A^H = A^H_{ideal} + A^H_{guest-guest}$, where A^H_{ideal} is the vdWP expression given in eq 1 and $A^H_{guest-guest}$ is the explicit contribution of the guest−guest interactions.

Acknowledgment. This research was sponsored by the Laboratory Directed Research and Development Program of Oak Ridge National Laboratory (ORNL), managed by UT-Battelle, LLC, for the U. S. Department of Energy under Contract DE-AC05-00OR22725.

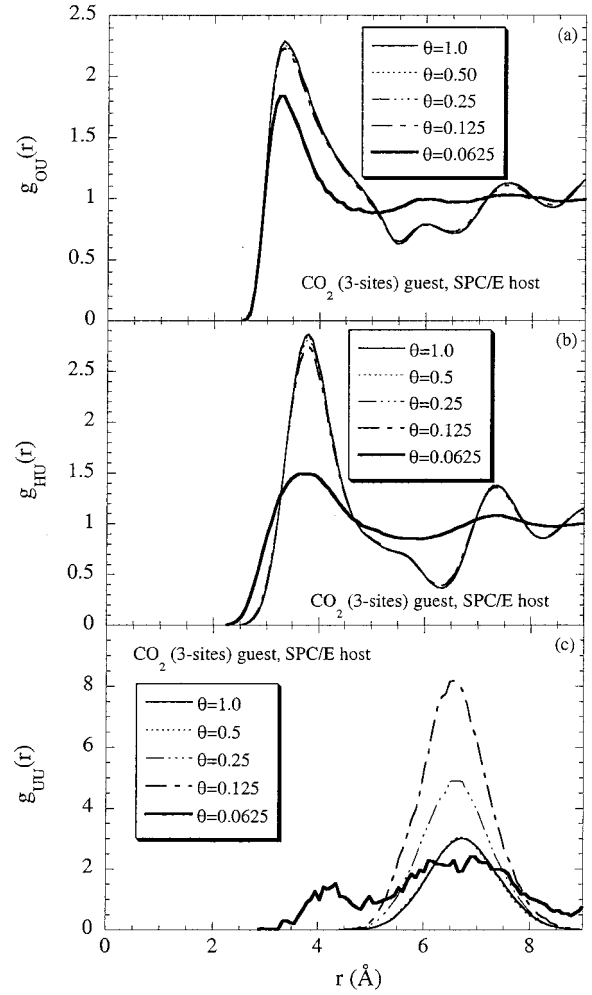

Figure 11. Isobaric−isothermal effect of host occupancy on the host−guest microstructure for the carbon dioxide hydrate described by the Harris−Yung potential for the guest and the SPC/E model for the host.

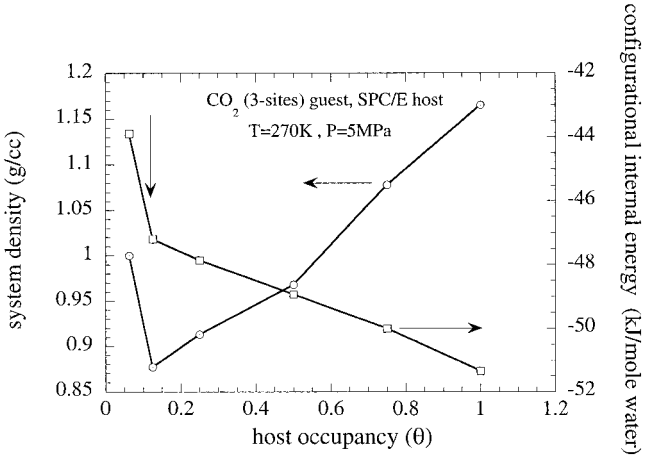

Figure 12. Isobaric−isothermal effect of host occupancy on the total configurational internal energy and density for the carbon dioxide hydrate described by the Harris−Yung potential for the guest and the SPC/E model for the host. The vertical arrow indicates the limit of hydrate stability.

Appendix. Translation of Williams' Methane Model to a Lennard-Jones-Type Model

The main goal here is to translate the original exp-6 radial dependence into a Lennard-Jones form, one that preserves two key parameters: the depth of the energy well ($-\epsilon$) and the soft-core diameter σ of the original representation.

Starting with the exp-6-type potential

$$\phi_{\alpha\beta}(r) = B_{\alpha\beta}\exp(-C_{\alpha\beta}r) + A_{\alpha\beta}/r^6 \qquad \text{(A1)}$$

we determine the distance at which this potential exhibits its minimum, i.e.

$$[\partial\phi_{\alpha}\beta(r)/\partial r]_{r=r_{m}{}^{\alpha\beta}} = -C_{\alpha\beta}B_{\alpha\beta}\exp(-C_{\alpha\beta}r_{m}^{\alpha\beta}) - 6A_{\alpha\beta}/(r_{m}^{\alpha\beta})^7 = 0 \qquad \text{(A2)}$$

such that

$$[\partial^2\phi_{\alpha\beta}(r)/\partial r^2]_{r=r_{m}{}^{\alpha\beta}} > 0 \qquad \text{(A3)}$$

Obviously, from eqs A1 and A2, we also have that

$$\phi_{\alpha\beta}(r=r_{m}^{\alpha\beta}) = B_{\alpha\beta}\exp(-C_{\alpha\beta}r_{m}^{\alpha\beta}) - A_{\alpha\beta}/(r_{m}^{\alpha\beta})^6 = -\epsilon_{\alpha\beta} \qquad \text{(A4)}$$

so that, from eqs A2 and A4, we obtain

$$\epsilon_{\alpha\beta} = \left[\frac{A_{\alpha\beta}}{(r_{m}^{\alpha\beta})^6}\right]\left(\frac{6}{C_{\alpha\beta}r_{m}^{\alpha\beta}} - 1\right) \qquad \text{(A5)}$$

Moreover, eq A1 becomes zero at $r = \sigma_{\alpha\beta}$, i.e.

$$\phi_{\alpha\beta}(\sigma_{\alpha\beta}) = B_{\alpha\beta}\exp(-C_{\alpha\beta}\sigma_{\alpha\beta}) + A_{\alpha\beta}/(\sigma_{\alpha\beta})^6 = 0 \qquad \text{(A6)}$$

Therefore, for a given set of ($A_{\alpha\beta}$, $B_{\alpha\beta}$, $C_{\alpha\beta}$) parameters, eq A6 can be solved by iteration to obtain the corresponding value of $\sigma_{\alpha\beta}$. Then, recalling that $r_{m}^{\alpha\beta} > \sigma_{\alpha\beta}$, we can solve eq A2, starting with $\sigma_{\alpha\beta}$ as the first approximation for the solution and avoiding the other possible root $r = r_{max}^{\alpha\beta} \ll \sigma_{\alpha\beta}$ that corresponds to the maximum of $\phi_{\alpha\beta}(r)$. Finally, by introducing the calculated value of $r_{m}^{\alpha\beta}$ into eq A5, we can determine $\epsilon_{\alpha\beta}$.

Here, a note of caution is necessary. Recently,[57] it was proposed that the "translation" of an exp-6 potential to a Lennard-Jones form could be achieved by rewriting eq A1 as

$$\phi_{\alpha\beta}(r) = 4\epsilon_{\alpha\beta}\{\exp[C_{\alpha\beta}(\sigma_{\alpha\beta} - r)] - \sigma_{\alpha\beta}/r^6\} \qquad \text{(A7)}$$

so that $B_{\alpha\beta} = 4\epsilon_{\alpha\beta}\exp(C_{\alpha\beta}\sigma_{\alpha\beta})$ and $A_{\alpha\beta} = -4\epsilon_{\alpha\beta}\sigma_{\alpha\beta}{}^6$. Even though eq A7 obeys the condition that $\phi_{\alpha\beta}(r=\sigma_{\alpha\beta}) = 0$, it is not possible to impose the Lennard-Jones constraint $2^{1/6}\sigma_{\alpha\beta} = r_{m}^{\alpha\beta}$ to determine the value of $\epsilon_{\alpha\beta}$ as was done by Koneshan and Rasaiah,[57] i.e.

$$C_{\alpha\beta}\sigma_{\alpha\beta} = -(\ln 4)/(1 - 2^{1/6}) = 11.320 \ldots \qquad \text{(A8)}$$

$$\epsilon_{\alpha\beta} = 0.25B_{\alpha\beta}\exp[(\ln 4)/(1 - 2^{1/6})] \qquad \text{(A9)}$$

$$\sigma_{\alpha\beta} = \{(-A_{\alpha\beta}/B_{\alpha\beta})\exp[-(\ln 4)/(1 - 2^{1/6})]\}^{1/6} \qquad \text{(A10)}$$

because the relationship between $\sigma_{\alpha\beta}$ and $r_{m}^{\alpha\beta}$ depends on $C_{\alpha\beta}$, i.e., $\sigma_{\alpha\beta} \equiv f(r_{m}^{\alpha\beta}, C_{\alpha\beta})$ (see ref 58), and consequently, the value of $\sigma_{\alpha\beta}$ determined according to eq A10 will not necessarily satisfy $\phi_{\alpha\beta}(\sigma_{\alpha\beta}) = 0$.

References and Notes

(1) van der Waals, J. H.; Platteeuw, J. C. Clathrate Solutions. In *Advances in Chemical Physics*; Prigogine, I., Ed.; Interscience Publishers: New York, 1959; Vol. 2, pp 1−58.
(2) MacDonald, G. J. *Annu. Rev. Energy* **1990**, *15*, 53−83.
(3) Kvenvolden, K. A. *Org. Geochem.* **1995**, *23*, 997−1008.
(4) Kvenvolden, K. A. *Chem. Geol.* **1988**, *71*, 41−51.
(5) Taylor, F. W. *Rep. Prog. Phys.* **1991**, *54*, 881−918.

(6) Bell, P. R. Methane Hydrate and the Carbon Dioxide Question. In *Carbon Dioxide Review*; Clark, W. C., Ed.; Oxford University Press: New York, 1982; pp 401−406.
(7) Brewer, P. G.; Orr, F. M.; Friederich, G.; Kvenvolden, K. A.; Orange, D. L. *Energy Fuels* **1998**, *12*, 183−188.
(8) van der Waals, J. H. *Faraday Soc. Discuss.* **1953**, *15*, 261−262.
(9) van der Waals, J. H. *Trans. Faraday Soc.* **1956**, *52*, 184−193.
(10) van der Waals, J. H. *Ann. N. Y. Acad. Sci.* **1994**, *715*, 29−39.
(11) Sloan, E. D. *Clathrate Hydrates of Natural Gases*, 2nd ed.; Marcel Dekker: New York, 1998.
(12) Lennard-Jones, J. E.; Devonshire, A. F. *Proc. R. Soc. London* **1937**, *A163*, 53−70.
(13) Berendsen, H. J. C.; Postma, J. P. M.; van Gunsteren, W. F.; Hermans, J. Interaction Models for Water in Relation to Protein Hydration. In *Intermolecular Forces: Proceedings of the Fourteenth Jerusalem Symposium on Quantum Chemistry and Biochemistry*; Pullman, B., Ed.; Reidel: Dordrecht, The Netherlands, 1981; pp 331−342.
(14) Jorgensen, W. L. *J. Am. Chem. Soc.* **1981**, *103*, 335−340.
(15) Teleman, O.; Jönsson, B.; Engström, S. *Mol. Phys.* **1987**, *60*, 193−203.
(16) Rodger, P. M. *AIChE J.* **1991**, *37*, 1511−1516.
(17) Førrisdahl, O. K.; Kwamme, B.; Haymet, A. D. J. *Mol. Phys.* **1996**, *89*, 819−834.
(18) Hirai, S.; Okazaki, K.; Tabe, Y.; Kawamura, K. *Energy Convers. Manage.* **1997**, *38*, S301−S306.
(19) Berendsen, H. J. C.; Grigera, J. R.; Straatsma, T. P. *J. Phys. Chem.* **1987**, *91*, 6269−6271.
(20) Mahoney, M. W.; Jorgensen, W. L. *J. Chem. Phys.* **2000**, *112*, 8910−8922.
(21) de Pablo, J. J.; Prausnitz, J. M.; Strauch, H. J.; Cummings, P. T. *J. Chem. Phys.* **1991**, *93*, 7355−7359.
(22) Guissani, Y.; Guillot, B. J. *J. Chem. Phys.* **1993**, *98*, 8221−8235.
(23) Jorgensen, W. L.; Madura, J. D.; Swenson, C. J. *J. Am. Chem. Soc.* **1984**, *106*, 6638−6646.
(24) Williams, D. E. *J. Chem. Phys.* **1967**, *47*, 4680−4684.
(25) Murad, S.; Evans, D. J.; Gubbins, K. E.; Streett, W. B.; Tildesley, D. J. *Mol. Phys.* **1979**, *37*, 725−736.
(26) Habenschuss, A.; Johnson, E.; Narten, A. H. *J. Chem. Phys.* **1981**, *74*, 5234−5241.
(27) Chen, B.; Martin, M. G.; Siepmann, J. I. *J. Phys. Chem. B* **1998**, *102*, 2578−2586.
(28) Panagiotopoulos, A. Z. *Mol. Phys.* **1987**, *61*, 813−826.
(29) Reid, R. C.; Prausnitz, J. M.; Sherwood, T. K. *The Properties of Liquids and Gases*, 3rd ed.; McGraw-Hill: New York, 1977.
(30) Harris, J. G.; Yung, K. H. *J. Phys. Chem.* **1995**, *99*, 12021−12024.
(31) Nosé, S. *Mol. Phys.* **1984**, *52*, 255−268.
(32) Andersen, H. C. *J. Chem. Phys.* **1980**, *72*, 2384−2393.
(33) Gear, C. W. *The Numerical Integration of Ordinary Differential Equations of Various Orders*; Argonne National Laboratory: Argonne, IL, 1966.
(34) Allen, M. P.; Tildesley, D. J. *Computer Simulation of Liquids*; Oxford University Press: New York, 1987.
(35) Evans, D. J.; Murad, S. *Mol. Phys.* **1977**, *34*, 327−331.
(36) Neumann, M. *Mol. Phys.* **1983**, *50*, 841−858.
(37) McMullan, R. K.; Jeffrey, G. A. *J. Chem. Phys.* **1965**, *42*, 2725−2737.
(38) Bernal, J. D.; Fowler, R. H. *J. Chem. Phys.* **1933**, *1*, 515−547.
(39) Chialvo, A. A.; Cummings, P. T.; Simonson, J. M.; Mesmer, R. E.; Cochran, H. D. *Ind. Eng. Chem. Res.* **1998**, *37*, 3021−3025.
(40) Chialvo, A. A.; Yezdimer, E.; Driesner, T.; Cummings, P. T.; Simonson, J. M. *Chem. Phys.* **2000**, *258*, 109−120.
(41) Chialvo, A. A.; Cummings, P. T. Molecular-based Modeling of Water and Aqueous Solutions at Supercritical Conditions. In *Advances in Chemical Physics*; Rice, S. A., Ed.; Wiley & Sons: New York, 1999; Vol. 109, pp 115−205.
(42) Belosludov, V. R.; Lavrentiev, M. Y.; Dyadin, Y. A. *J. Inclusion Phenom. Mol. Recognit. Chem.* **1991**, *10*, 399−422.
(43) Rodger, P. M. *J. Phys. Chem.* **1989**, *93*, 6850−6855.
(44) Rodger, P. M. *J. Phys. Chem.* **1990**, *94*, 6080−6089.
(45) Dharmawardhana, P. B.; Parrish, W. R.; Sloan, E. D. *Ind. Eng. Chem. Fundam.* **1980**, *19*, 410−414.
(46) Tester, J. W.; Bivins, R. L.; Herrick, C. C. *AIChE J.* **1972**, *18*, 1220−1230.
(47) John, V. T.; Holder, G. D. *J. Phys. Chem.* **1981**, *85*, 1811−1814.
(48) John, V. T.; Holder, G. D. *J. Phys. Chem.* **1982**, *86*, 455−459.
(49) John, V. T.; Papadopoulos, K. D.; Holder, G. D. *AIChE J.* **1985**, *31*, 252−259.
(50) John, V. T.; Holder, G. D. *J. Phys. Chem.* **1985**, *89*, 3279−3285.
(51) Sparks, K. A. Configurational Properties of Water Clathrates through Molecular Simulation. Ph.D. Massachusetts Institute of Technology, Cambridge, MA, 1991.
(52) Sparks, K. A.; Tester, J. W. *J. Phys. Chem.* **1992**, *96*, 11022−11029.
(53) Sparks, K. A.; Tester, J. W.; Cao, Z.; Trout, B. L. *J. Phys. Chem. B* **1999**, *103*, 6300−6308.
(54) Prausnitz, J. M.; Lichtenthaler, R. N.; de Azevedo, E. G. *Molecular Thermodynamics of Fluid Phase Equilibria*, 2nd. ed.; Prentice Hall: Englewood Cliffs, NJ, 1986.
(55) Sitarski, M. *Rocz. Chem.* **1975**, *49*, 159−164.
(56) Istomin, V. A. *Russ. J. Phys. Chem.* **1987**, *61*, 1987−1988.
(57) Koneshan, S.; Rasaiah, J. C. *J. Chem. Phys.* **2000**, *113*, 8125−8137.
(58) Hirschfelder, J. O.; Curtiss, C. F.; Bird, R. B. *Molecular Theory of Gases and Liquids*; Wiley and Sons, Inc.: New York, 1954.